Analysis of Amylbenzene Adsorption Equilibria on Different RP-HPLC

Malgorzata Gubernak[1], Wojciech Zapala[1], Krystyna Tyrpien[2], and **Krzysztof Kaczmarski[1,*]**

[1]Faculty of Chemistry, Rzeszów University of Technology, W. Pola 2 Street, 35-959, Rzeszów and [2]Department of Chemistry, Medical University of Silesia, Zabrze, Poland

Abstract

For the purpose of description of the adsorption process of amylbenzene on a C_8-, C_{18}-, and C_{30}-bonded silica stationary phase with methanol–water (80:20, v/v) as the mobile phase, a novel adsorption model (called the cluster isotherm model) is used. The model assumes the possibility of independent adsorption of analyte clusters on the longer C_{30} and shorter C_8 chains. The validation of the proposed isotherm is made by comparison of experimental breakthrough and peak profiles obtained for RP-8e and RP-30 columns at a temperature of 24°C and for RP-18e at a temperature range of 7–60°C, with a theoretical simulation using the Transport-Dispersive model.

Introduction

Preparative liquid chromatography (LC) remains one of the most important processes for the separation and purification of biological products despite the development of other separation methods. For economic reasons, preparative chromatography must be performed at high concentrations (1), under which conditions the equilibrium is nonlinear. Generally, in preparative chromatography, the equilibrium isotherms are usually Langmuirian-shaped (concave downward), which suggests the formation of a simple monolayer. Rarely, the adsorption equilibrium in a liquid-solid system can apply S-shaped isotherms (concave upward). This type of isotherm model is frequently observed in gas–solid chromatography when multilayer adsorption takes place. The curvature of S-shaped isotherms at the origin and at low concentrations is concave upward, which indicates that the amount adsorbed at equilibrium increases more rapidly than the concentration in the mobile phase. S-shaped isotherms are also theoretically possible when lateral interaction between adsorbed molecules have a major impact on sorption thermodynamics. Such models, for example, are the Fowler–Guggenheim and Fowler–Guggenheim–Jovanovic isotherms (2,3).

S-shaped isotherms were recently observed for adsorption of butylbenzene and amylbenzene on Chromolith Performance monolithic silica columns (Merck, Darmstadt, Germany) by Cavazzini et al. (4). The best isotherm model found for the alkylbenzenes was the anti-Langmuir isotherm, whereas for butyl benzoate the liquid–solid state version of the Brunauer–Emmet–Teller (B.E.T.) isotherm was better (5). There, isotherm models should be treated as a good mathematical approximation of experimental data rather than a description of the physical process. The anti-Langmuir isotherm has no physical interpretation, whereas the B.E.T. isotherm is obtained by assuming an infinite number of adsorbed layers of the species.

Validation of the proposed isotherms was achieved by comparison of theoretical breakthrough curves or peak profiles with those observed experimentally. However, the relatively good agreement was obtained between theoretical and experimental peak profiles of alkylbenzenes only for a limited range of concentrations (4). Butyl benzoate agreement between experimental and theoretical breakthrough curves was better, although in order to achieve a good description of experimental data, the number of theoretical plates had to be adjusted to each concentration profile separately (5,6). The comparison between experiment and theory was performed using of a simple Equilibrium-Dispersive model or a more complicated POR model (4–6).

Previously, the adsorption process of amylbenzene on LiChrospher RP-18e column using a novel adsorption model called the cluster isotherm model was investigated at constant temperature equal 24°C (7). It was shown that the cluster isotherm model very accurately describes the adsorption behavior of this compound. The validity of this cluster isotherm model was supported by very good agreement between the experimental breakthrough profiles recorded and those calculated for the full range of mobile phase inlet concentration: from the minimum possible to saturation concentration. This agreement was achieved using for the calculations the GR and Equilibrium-Dispersive models. The agreement between concentration profiles generated by both models are very similar, which suggests that breakthrough shape profiles depends mainly on sorption thermodynamics, and the influence of mass transfer resistances on outlet concentration profiles has a secondary effect.

The main goal of this study was to validate the novel cluster

* Author to whom correspondence should be addressed: email kkaczmarski@prz.rzeszow.pl.

isotherm model (7) on the C_8 and C_{30} adsorbent with and without endcapping. The experiments were performed at a temperature of 24°C. Additionally, we have performed new experiments on an RP-18e column at temperatures of 7°C, 40°C, and 60°C. The validation of the analyzed isotherm was made by comparing the experimental peak and breakthrough profiles with theoretical simulations using the Transport-Dispersive (TD) model.

Theory

Mass transport equation

The TD model was used in this work. This model is frequently used when the mass transfer resistances have a moderate influence on the profiles of chromatographic bands. This model consists of the mass transport equation for the mobile phase:

$$\frac{\partial C_i}{\partial t} + F\frac{\partial q_i}{\partial t} + \frac{u}{\varepsilon_t}\frac{\partial C_i}{\partial z} = \frac{\varepsilon_e}{\varepsilon_t} D_L \frac{\partial^2 C_i}{\partial z^2} \qquad \text{Eq. 1}$$

and the mass transfer kinetic equation:

$$\frac{\partial q_i}{\partial t} = k_f[q_i^*(C) - q_i] \qquad \text{Eq. 2}$$

where q_i^* is the concentration in the adsorption monolayer at the adsorbent surface in equilibrium with the concentration C_i in the mobile phase, q_i is a species concentration, u is superficial velocity, D_L is dispersion coefficient, and e_e and e_t are the bed and total porosities.

The coefficient k_f in TD model was established from equation (3) to obtain consistency with the General Rate (GR) model solution (8):

$$k_f = k\cdot(1-\varepsilon_e)\frac{3}{R}\left(\frac{k_0'}{1+k_0'}\right)^2 \Big/ k_0'\varepsilon_t\left(\frac{k_1}{1+k_1}\right)^2 \qquad \text{Eq. 3}$$

where the coefficients k_0' and k_1 were calculated by means of the following expressions:

$$k_o' = \frac{1-\varepsilon_t}{\varepsilon_t}\frac{\Delta q}{\Delta C} \qquad \text{Eq. 4}$$

$$k_1 = \frac{1-\varepsilon_e}{\varepsilon_e}\left[\varepsilon_p + (1-\varepsilon_p)\frac{\Delta q}{\Delta C}\right] \qquad \text{Eq. 5}$$

The quotient, $\frac{\Delta q}{\Delta C}$, was calculated for local liquid phase concentration.

The overall mass transfer coefficient, k, is given by the following relationship:

$$k = \left[\frac{1}{k_{ext}} + \frac{1}{k_{int}}\right]^{-1} \qquad \text{Eq. 6}$$

where k_{ext} and k_{int} are the external and the internal mass transfer coefficients, respectively. The internal mass transfer coefficients are obtained from the equations:

$$k_{int} = \frac{10 D_{eff}}{d_p} \qquad D_{eff} = \frac{\varepsilon_p D_m}{\gamma} \qquad \gamma = \frac{1}{\varepsilon_p} \qquad \text{Eq. 7}$$

where D_m is the molecular diffusivity, g is the tortuosity factor, and e_p is particle porosity.

Equations 1–7 were solved with well-known Danckwerts boundary conditions. The concentration of the species in the column was assumed to be equal zero for time $t < 0$.

The model was solved using a computer program based on an implementation of the method of orthogonal collocation on finite elements (1,9,10). The set of discretized ordinary differential equations were solved with the Adams–Moulton method, implemented in the variable coefficient ODE solver (VODE) procedure (11). The relative and absolute errors of the numerical calculations were 1×10^{-6} and 1×10^{-8}, respectively.

Models of adsorption isotherms

In a chromatographic system, the behavior of the solute is characterized by the equilibrium isotherm, which is the relationship between the concentrations of this compound in the stationary and mobile phase at equilibrium. The equilibrium data [$q = f(C)$] for amylbenzene were fitted to different models of adsorption isotherms for liquid–solid equilibrium. Only those models that best account for liquid–solid equilibrium data are considered here. These are the B.E.T. (12) and the cluster isotherm models (7).

The B.E.T. isotherm is depicted by equation:

$$q = q_s\frac{K_1 C}{(1-K_a C)(1-K_a C + K_1 C)} \qquad \text{Eq. 8}$$

where q_s is the saturation capacity, K_1 is the equilibrium constant that depicts equilibrium between the active site and first adsorption layer, and K_a is the equilibrium constant that depicts the equilibrium between the previous and next analyte layer.

The cluster isotherm is defined by the following relationships:

$$q_1 = \frac{q_s * K_1 * C}{D} \qquad \text{Eq. 9}$$

$$q_2 = \frac{q_s * K_1 * K_2 * C^2}{D} \qquad \text{Eq. 10}$$

$$q_n = \frac{q_s * K_1 * K_n * C^n}{D} \qquad \text{Eq. 11}$$

where:

$$D = 1 + K_1 * C + K_1 * K_2 * C^2 + \ldots + K_1 * K_n * C^n = 0 \qquad \text{Eq. 12}$$

The total concentration of adsorbed molecules is equal:

$$q = q_1 + 2 * q_2 + \ldots + n * q_n \qquad \text{Eq. 13}$$

The equilibrium constant, K_i, represents the effective equilibrium for process cluster formation and adsorption.

Detector calibration

In order to interpret the experimental data, the signal coming from the detector has to be converted to the concentration units.

To do that, first the calibration curve of the detector has be established. In the case of the breakthrough profiles, the dependence between the response of the detector and the concentration can be read directly from the signal corresponding to the concentration plateau. However, using the calibration curve from the breakthrough experiment in order to convert signal of the detector to concentration often brings incorrect results. The calculated mass of the species contained in the effluent can be considerably different from the experimental aliquot introduced to the column (see equation 14). It is attributable to the fact that the signal from the detector changes quasi-periodically over the longer periods of time. Cavazzini et al. determined the calibration curve after having measured all the overload profiles (4) and found out that the repeatability between different calibration curves was not higher than 5%. The same problem was also observed in our experiment. It is noteworthy that small errors in establishing of the calibration curves can result in much higher errors when calculating concentrations and, particularly, for higher concentrations when the sensitivity of detection is affected considerably.

In this study, the calibration curve was indirectly measured from the mass balance equation. The mass of the species introduced to the column should equal to that at the column outlet:

$$C^o \cdot t_p \cdot u \cdot A = \int_0^\infty u \cdot A \cdot C(t) \cdot dt \qquad \text{Eq. 14}$$

where C^o is the inlet concentration, t_p is the time needed by the analyzed species to be introduced to the column, $C(t)$ is the concentration at the column outlet at time t (calculated using the calibration curve), u is the superficial velocity, and A is the surface of the cross-section of the column. Alternatively we can write:

$$C^0 t_p = \int_0^\infty C(t)dt \qquad \text{Eq. 14a}$$

Let us assume, that in n experiments with different inlet concentrations (C^0_i, i = 1,2,...n), the different peak profiles for one and the same species were measured. For each single concentration, equation 14a should be fulfilled. This equation can be rewritten as follows:

$$C_i^o t_p = \int_o^\infty C(S_i(t))dt, \ i = 1,...,n \qquad \text{Eq. 15}$$

where $C(S_i(t))$ is the dependence of concentration on the detector response, S (calibration curve), and the subscript i denotes the i-th experiment.

The calibration curve can be virtually any thinkable function, but in this study we assumed a frequently used polynomial dependence between concentration and the detector response [$C(S(t)) = p_1*S(t)+ p_2*S(t)^2+p_3*S(t)]^3$. Thus equation 15 can be rewritten, as follows:

$$C_i^o \cdot t_p = \int_0^\infty (p_1 \cdot S_i(t) + p_2 \cdot S_i(t)^2 + p_3 \cdot S_i(t)^3) \cdot dt, \ i = 1,...,n \qquad \text{Eq. 16}$$

After having introduced the experimentally measured detector response $S_i(t)$ (i = 1,…n) to equation 16, the set of n integral equations was obtained. Finally, in order to obtain the explicit equation for the calibration curve, the parameters p_i were estimated using the Marquardt method of the least-squares, modified by Fletcher (13). The integral in equation 16 was calculated with the aid of the trapezoid method.

Experimental

Chemicals

The mobile phase used in this work was a mixture of 80% methanol–20% water (v/v). The analyte was the amylbenzene. For the measurements of the dead column time, uracil was used. All the chemicals were purchased from Merck. The mobile phase flow rate was 1.0 cm^3/min in all experiments.

Column

The LiChroCart, LiChrospher 100 (RP-18e and RP-8e, 125 × 4.0 mm, 5 µm) column from Merck was used in all experiments. Moreover, the experiments were performed on the RP-30 column (250 × 4.0 mm) from the Institute of Organic Chemistry of the University of Tübingen (Tübingen, Germany). The hold-up time determined by the retention time of uracil was 0.939, 1.08, and 2.707 min, respectively, for the mentioned columns. The total porosity calculated from the hold-up time was e_t of 0.598, 0.688, and 0.862.

Apparatus

The data were acquired using a Merck–Hitachi chromatograph model LaChrom assembled from L-7100 pump, L-7455 diode array detector, D-7000 interface, L-7350 column oven, and L-7612 solvent degasser. The absorbance was measured at 272.1 nm. The measurements were carried out at the constant temperature of 24°C for columns RP-8e and RP-30 and at the temperatures of 7°C, 40°C, and 60°C for column RP-18e.

Results and Discussion

Determination of the amylobenzene isotherm model by frontal analysis method for different columns

In this work, the adsorption data of amylbenzene were derived from the frontal analysis data (1). The equilibrium concentration was calculated using the equal area method. The adsorbed amount of amylbenzene, q^*, was calculated assuming that the total porosity depends of the mobile phase concentration. These calculations were made by use of the following equation:

$$q = \frac{V_r(C) - V_o(C)}{V_a} \cdot C = \frac{V_r(C) - V_0(C)}{V_0(C)} \cdot \frac{V_0(C)}{V_a} \cdot C \qquad \text{Eq. 17}$$

where $V_0(C)$ is the hold-up volume, measured by recording the retention time of a nonretained compound at the plateau concentration; V_a is the volume of the stationary phase; V_r is the retention volume of the breakthrough curve; and q is the concentration in the solid phase at equilibrium with the plateau concentration in the fluid phase.

After some mathematical simplification, equation 17 can be written:

$$q = \frac{t_r(C) - t_0(C)}{t_0(C)} \cdot \frac{\varepsilon_t(C)}{(1-\varepsilon_t^0)} \cdot C \qquad \text{Eq. 18}$$

where $t_0(C)$ is the hold-up retention time; $e_t(C)$ is the total porosity, which depends on the plateau concentration, C; and e_t^0 is the total porosity when the column is equilibrated with the pure mobile phase (for a plateau concentration equal to zero).

Finally the equilibrium concentration of amylbenzene was calculated using equation 18. The changes of porosity were neglected in mass transport equation 1 because of its negligible influence on calculated band profiles, as it was proved previously using the GR model (7).

Verification of the isotherm models for various type of columns

In a previous study (7) it was found that the equilibrium isotherm of amylbenzene on the RP-18e column was concave upward and fit well to the cluster isotherm model. The best numerical values of the cluster and B.E.T. isotherm model studied in this work were estimated by fitting the experimental adsorption data obtained with frontal analysis to the models equation using the least-squares Marquardt method modified by Fletcher (13) for columns RP-8e and RP-30 at a temperature of 24°C and for RP-18e column at different temperatures. Only the values of equilibrium constants (K_1, K_2,…) were estimated. The saturation capacity, q_s, was obtained from the calculated value of the Henry constant ($H = q_s \times K_1$). The value of the Henry constant was calculated from the retention time, t_r, of peak profiles obtained at very low concentration.

$$t_r = \frac{L \cdot \varepsilon_t}{u}\left(1 + \frac{1-\varepsilon_t}{\varepsilon_t} \cdot H\right) \qquad \text{Eq. 19}$$

where L is the column height.

The calculated values of the Henry constant (H) for columns RP-8e, RP-18e, and RP-30 were equal to 7.95, 13.92, and 21.056. The best estimates of the parameters of the isotherms (discussed in the Models of adsorption isotherm section) are reported in Table I for RP-8e and RP-30. Table II lists the best parameters of the isotherm models for the RP-18e column at different temperatures. In this case, it was assumed that the saturation capacity for different temperatures was the same as for 24°C. The data for 24°C were taken from a previous paper (7).

The conclusions that follow from the data presented in Tables I and II are consistent with the expectation that the saturation capacities and equilibrium constants increase with ligand-length increase, and the equilibrium constants decrease with temperatures. These results hold for both analyzed isotherms. The maximum amount of amylbenzene particles in clusters, predicted by cluster isotherm, was generally four. We had to assume clusters coupled from up to six molecules at a temperature of 7°C in order to obtain good agreement in the experiment.

Table I. The Best Value Parameters of the Isotherm Models

Column temp.	B.E.T. isotherm	Cluster isotherm
RP-8e (t = 24°C)	q_s = 114.6	q_s = 450.7
	K_1 = 0.06937	K_1 = 0.01764
	K_2 = 0.05245	K_2 = 0.03015
	–	K_3 = 0
	–	K_4 = 0.0001545
RP-30 (t = 24°C)	q_s = 190.9	q_s = 496.9
	K_1 = 0.1103	K_1 = 0.04237
	K_2 = 0.06388	K_2 = 0.3451
	–	K_3 = 0
	–	K_4 = 0.0003061

Table II. The Best Value Parameters of the Isotherm Models for the RP-18e Column at Different Temperatures

Temperature	B.E.T. isotherm	Cluster isotherm
RP-18e (t = 7°C)	q_s = 150.8	q_s = 469
	K_1 = 0.1402	K_1 = 0.0381
	K_2 = 0.0586	K_2 = 0.0371
	–	$K_3 = K_4 = K_5 = 0$
	–	$K^6 = 4.336 \times 10^{-6}$
RP-18e (t = 24°C)	q_s = 150.8	q_s = 468.7
	K_1 = 0923	K_1 = 0.0297
	K_2 = 0.0482	K_2 = 0.203
	–	K_3 = 0
	–	K_4 = 0.00011
RP-18e (t = 40°C)	q_s = 150.8	q_s = 469
	K_1 = 0.06330	K_1 = 0.0204
	K_2 = 0.03473	K_2 = 0.01389
	–	K_3 = 0
	–	$K_4 = 4.41 \times 10^{-5}$
RP-18e (t = 60°C)	q_s = 150.8	q_s = 469
	K_1 = 0.04346	K_1 = 0.0146
	K_2 = 0.02325	K_2 = 0.004822
	–	K_3 = 0
	–	$K_4 = 2.4 \times 10^{-5}$

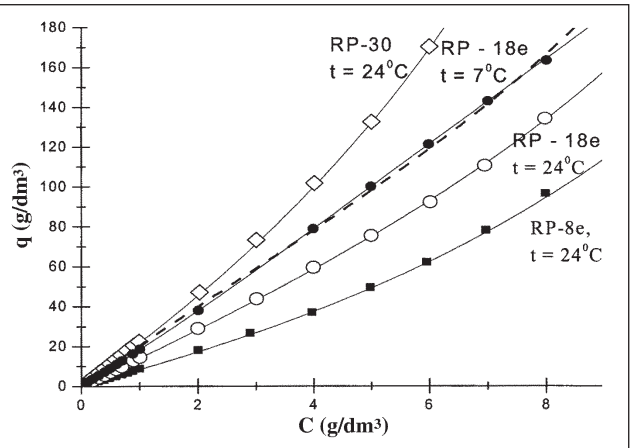

Figure 1. Comparison between the experimental isotherm data (symbols) obtained for different columns and the cluster isotherm with the values of the parameters in Table I and II (solid line). The dashed line for temperature equal 7°C represent the B.E.T. model.

Figure 1 contains a comparison of the experimental adsorption data (symbols), which were obtained for various types of packed columns, with the cluster isotherm. The obtained agreement is excellent. Very similar agreement was obtained for the B.E.T. isotherm for all temperatures except 7°C. When the temperature was equal 7°C, there were visible differences between B.E.T. isotherm and experimental data.

Validation of the isotherm models

In chromatography, the validation of an isotherm model requires the calculation of overloaded band profiles under well-specified experimental conditions and the comparison of the results with experimental profiles recorded under these conditions. The choice of the best isotherm model to fit the experimental data must be made on this basis.

Breakthrough profiles

It was previously shown (7) that the GR and Equilibrium-Dispersive models coupled with the cluster or B.E.T. isotherm allow for an excellent prediction of the breakthrough curves. The agreement obtained between the experimental breakthrough profiles and simulated profiles were very good for analysis in this study (RP-18e column in temperature T equal to 24°C).

In this work, the validation of the isotherm models was made by comparison of experimental breakthrough profiles obtained for columns RP-8e and RP-30 in T = 24°C with theoretical simulation using the TD model discussed in the Mass transport equation section. The model is fully compatible with the GR model if the mass transfer resistances are not extremely low. The values of the parameters used in the TD model are listed in Table III. The value of the axial dispersion coefficient for different columns was calculated by use of the Gunn equation (14), assuming that the variance distribution of the ratio between the fluid linear velocity and the average velocity over the column cross-section was zero. The Wilke-Chang (15) correlation, as extended to mixed solvents by Perkins and Geankopolis (16), was used to calculate the molecular diffusion coefficient of amylbenzene in the mobile phase. The mass-transfer coefficient was calculated from the Wilson and Geankopolis correlation (17).

Table III. The Values of the Parameters Used in the TD Model of Chromatography

Parameter	Column RP-8e numerical value	Column RP-18e numerical value	Column RP-30 numerical value
Dispersion coefficient D_L (cm²/min)	0.00327	0.0032	0.00345
Molecular diffusion coefficient D_m (cm²/min)	0.00061	0.00061	0.00061
Superficial velocity (cm/min)	7.962	7.962	7.962
External mass transfer k_{ext} (cm/min)	6.68	6.68	6.68
Total porosity (ε_t)	0.688	0.598	0.862
External porosity (ε_e, assumed)	0.37	0.37	0.37
Internal porosity (ε_p)	0.505	0.362	0.781
Toruosity parameter $\gamma = 1/\varepsilon_p$	1.980	2.76	1.280

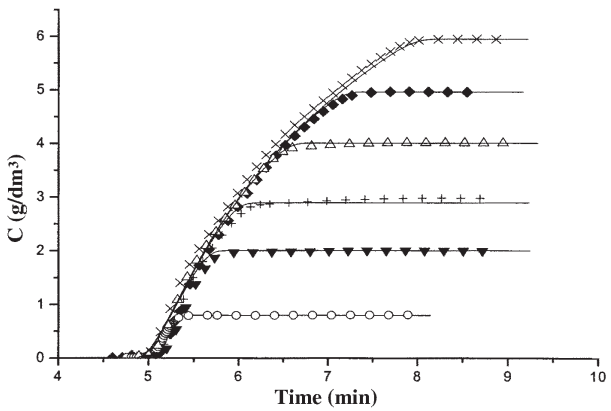

Figure 2. Comparison between chosen experimental breakthrough curves (symbols) and calculated breakthrough profiles (solid line) on the RP-8e column. The injection volume was 5 mL.

Figures 2 and 3 compare the experimental and calculated breakthrough profiles of amylbenzene for the RP-8e and RP-30 columns. The same excellent agreement was observed when the B.E.T. isotherm model was used for theoretical calculations (figures not presented).

Additionally, the theoretical isotherm models were validated by using it to calculate the breakthrough profiles of amylbenzene and comparing them to the experimental breakthrough curves obtained for column RP-18e in different temperatures (7°C, 24°C, 40°C, and 60°C). The agreement between calculated and experimental breakthrough profiles observed in Figure 4 shows that, for a temperature of 7°C, the cluster isotherm was remarkably more accurate in comparison with the B.E.T. isotherm. A small deviation between experimental isotherm data and B.E.T. model visualized in Figure 1 gives important differences between the experimental breakthrough profile and theoretical calculation for the B.E.T. isotherm. The bottom part of the calculated breakthrough profiles is typical for Langmuir-like isotherms, which is consistent with the shape of the bottom part of the B.E.T. isotherm approximation of the experimental equilibrium data.

For temperatures 24°C, 40°C, and 60°C, both isotherm models correctly describe of the experimental breakthrough profiles (figures not presented).

Peak profiles

For a final test of the validity of the isotherm models analyzed in this work, the experimental and theoretical peak profiles were compared. The peak concentration was calculated based on the detector response using a polynomial of the third degree as a calibration curve. The polynomial coefficients were estimated in the method described previously (Detector calibration section), for five experimental peaks presented in Figures 5 and 6, indepen-

dently. The mass balance error (see equation 14) was typically less than 1% and not greater than 2%.

The exemplary results of the comparison of band profiles obtained for RP-8e column and those calculated using the TD model coupled with the cluster isotherm are presented in Figures 5 and 6. Very similar results were obtained for the B.E.T isotherm. The elution profiles were taken for different injection times and concentrations. To emphasize the differences between experimental and theoretical peak profiles, the time scale was enlarged. The agreement between experimental and theoretical peak profiles were qualitatively good, the highs of peaks profiles were very similar. However, the slope of the experimental peak front was always steeper compared with the theoretical one. This observation suggests that the real adsorption process is probably more complicated than the analysis in the formulation of the cluster isotherm.

Conclusion

In this paper, the adsorption process of amylbenzene on RP-8e, RP-18e, and RP-30 adsorbent was investigated. The novel adsorption model assuming possibility of independent adsorption of analyte clusters on the C_8, C_{18}, and C_{30} chains was proposed. In contradiction to the B.E.T. isotherm, which assumes the formation of infinite numbers of analyte layers, the novel isotherm predicts interaction of generally only up to four molecules with one active site, which is more physically probable. The approximation of experimental data by the cluster and B.E.T. isotherms are generally very similar. However, only the cluster isotherm seems to make physical sense. The B.E.T. isotherm correctly describes the experimental breakthroughs profiles for 24°C, 40°C, and 60°C. However, when the temperature was 7°C, the approximation of breakthrough curve by cluster isotherm was remarkably more accurate in comparison with the B.E.T. isotherm (Figure 4), which seems to confirm the superiority of the cluster isotherm over the B.E.T. isotherm for the investigated adsorption process. For the simulation of breakthrough band, the TD model was used. Parameters of the TD model were calculated from appropriate correlations or measured from the independent experiment. The application of this model provided an excellent agreement between the experimental and calculated breakthrough curves for all columns used in this work.

The agreement between experimental and theoretical peak pro-

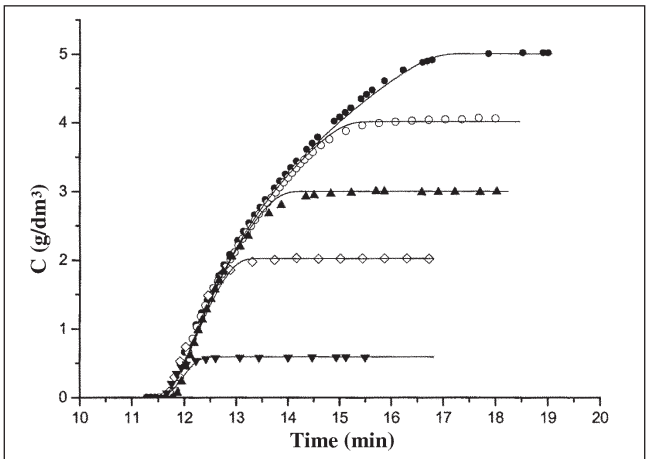

Figure 3. Comparison between chosen experimental breakthrough curves (symbols) and calculated breakthrough profiles (solid line) on the RP-30 column. The injection volume was 5 mL.

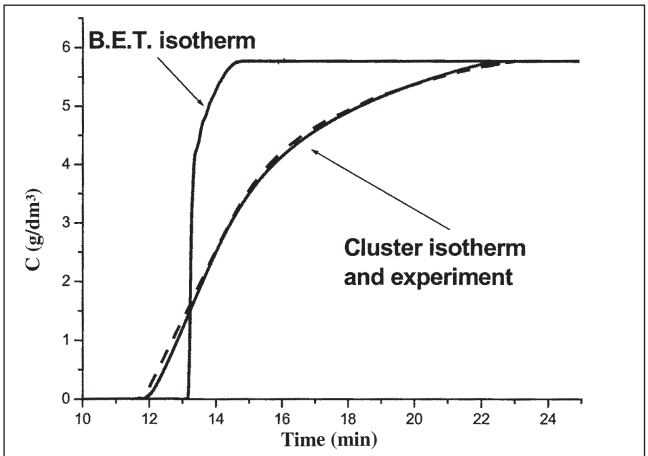

Figure 4. Comparison between the experimental (dashed line) and calculated (solid line) breakthrough profiles for B.E.T. and cluster isotherm models at a temperature of 7°C on the RP-18e column. The amylbenzene concentration was 6 g /dm³, and the injection volume was 5 mL.

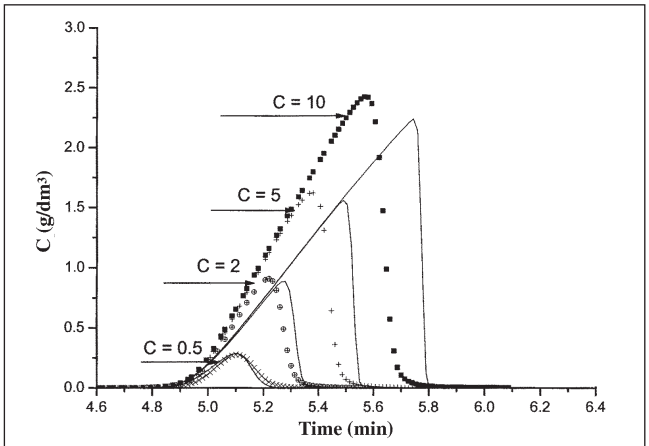

Figure 5. Comparison between experimental elution profiles (symbols) and theoretical profiles (solid line). The injection volume was 100 µL.

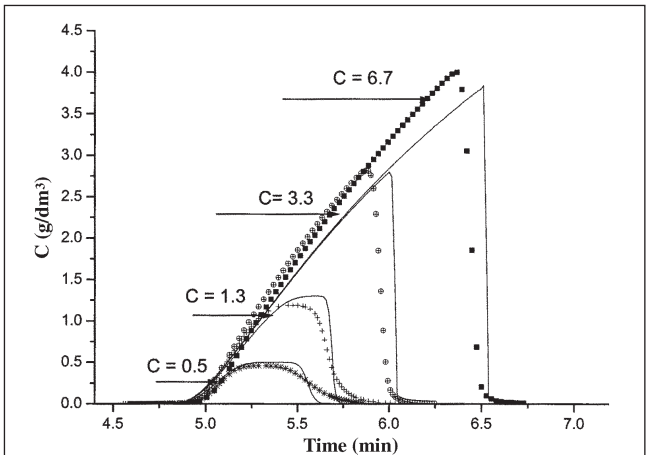

Figure 6. Comparison between experimental elution profiles (symbols) and theoretical profiles (solid line). The injection volume was 500 µL.

files was not as positive as for breakthrough curves. The main discrepancy was observed between the front slopes. The disagreement of the experimental and calculated elution peak profiles is difficult to explain but is probably connected with a more complicated adsorption mechanism than the one examined here.

Acknowledgments

This work was supported by Grant 4 T09C 006 23 of the Polish State Committee for Scientific Research. We thank Prof. Klaus Albert of the University of Tübingen for providing the new stationary phase synthesis and Dr. Stefan Bachmann for his help with C_{30} stationary phase preparation.

References

1. G. Guiochon, S.G. Shirazi, and A. Katti. *Fundamentals of Preparative and Nonlinear Chromatography*. Academic Press, Boston, MA, 1994.
2. R.H. Fowler and E.A. Guggenheim. *Statistical Thermodynamics*. Cambridge University Press, Cambridge, U.K., 1960.
3. I. Quinones and G. Guiochon. Extension of a Jovanovic–Freundlich isotherm model to multicomponent adsorption on heterogeneous surfaces. *J. Chromatogr. A* **796(1):** 15–40 (1998).
4. A. Cavazzini, G. Bardin, K. Kaczmarski, P. Szabelski, M. Al-Bokari, and G. Guiochon. Adsorption equilibria of butyl- and amylbenzene on monolithic silica-based columns. *J. Chromatogr. A* **957(2):** 111–26 (2002).
5. F. Gritti, W. Piatkowski, and G. Guiochon. Comparison of the adsorption equilibrium of a few low-molecular mass compounds on a monolithic and a packed column in reversed-phase liquid chromatography. *J. Chromatogr. A* **978(1-2):** 81–107 (2002).
6. F. Gritti, W. Piatkowski, and G. Guiochon. Study of the mass transfer kinetics in a monolithic column. *J. Chromatogr. A* **983(1-2):** 51–71 (2003).
7. M. Gubernak, W. Zapala, and K. Kaczmarski. Analysis of amylbenzene adsorption equilibria on an RP-18e chromatographic column. *Acta Chromatographica* **13:** 38–59 (2003).
8. K. Kaczmarski, D. Antos, H. Sajonz, P. Sajonz, and G. Guiochon. Comparative modeling of breakthrough curves of bovine serum albumin in anion-exchange chromatography. *J. Chromatography A* **925(1-2):** 1–17 (2001).
9. V.J. Villadsen and M.L. Michelsen. *Solution of Differential Equation Model by Polynomial Approximation*. Prentice-Hall, Englewood Cliffs, NJ, 1978.
10. A.J. Berninger, R.D. Whitley, X. Zhang, and N.-H.L. Wang. A versatile model for simulation of reaction and nonequilibrium dynamics in multicomponent fixed-bed adsorption process. *Comput. Chem. Eng.* **15:** 749 (1991).
11. P.N. Brown, A.C. Hindmarsh, and G.D. Byrne. VODE: a variable coefficient ODE solver. http:/www.netlib.org.
12. S. Brunauer, P.H.Emmet, and E. Teller. Adsorption of gases in multimolecular layers. *J. Am. Chem. Soc.* **60:** 309 (1938).
13. R. Fletcher. A modified Marquardt sub-routine for non-linear least squares. Tech. Report AERE R6788. U.K. Atomic Energy Authority Research Establishment, Harwell, U.K., 1971.
14. D. Gunn. Axial and radial dispersion in fixed beds. *J. Chem. Eng. Sci.* **42:** 363 (1987).
15. C.R. Wilke and P. Chang. Correlation of diffusion coefficients in dilute solution. *AIChE J.* **1:** 264 (1955).
16. L.R. Perkins and C.J. Geankoplis. Molecular diffusion in a ternary liquid system with the diffusing component dilute. *Chem. Eng. Sci.* **24:** 1035 (1969).
17. E.J. Wilson and C.J. Geankoplis. Liquid mass transfer and very low Reynolds number in packed beds. *Ind. Eng. Chem. Fund.* **5:** 9 (1966).

Manuscript accepted August 23, 2004.